Exploration of the Functional Site of a Scorpion α-like Toxin by Site-Directed Mutagenesis†

Chun-Guang Wang,[‡,§] Nicolas Gilles,[∥] Alain Hamon,[⊥] Frédéric Le Gall,[∥] Maria Stankiewicz,[⊥,@] Marcel Pelhate,[⊥] Yu-Mei Xiong,[‡,§] Da-Cheng Wang,*[,§] and Cheng-Wu Chi*[,‡]

Shanghai Institute of Biochemistry and Cell Biology, Chinese Academy of Sciences, Yue-Yang Road 320, Shanghai 200031, China, Institute of Biophysics, Chinese Academy of Sciences, Da-Tun Road 15, Beijing 100101, China, CEA, DIEP, Saclay, Gif-sur-Yvette, France, Laboratory of Neurophysiology, University of Angers, 2 Bd Lavoisier, 49045 Angers cedex, France, and Laboratory of Biophysics, N. Copernicus University, ul Gagarina 9, 87100 Torun, Poland

Received October 21, 2002; Revised Manuscript Received December 27, 2002

ABSTRACT: Scorpion α-neurotoxins can be classified into distinct subgroups according to their sequence and pharmacological properties. Using toxicity tests, binding studies, and electrophysiological recordings, BmK M1, a toxin from the Asian scorpion *Buthus martensi* Karsch, was experimentally identified as an α-like toxin. Being the first α-like toxin available in a recombinant form, BmK M1 was then modified by site-directed mutagenesis for investigation of the molecular basis of its activity. The results suggested a functional site which protrudes from the molecular scaffold as a unique tertiary arrangement, constituted by the five-residue reverse turn 8−12 and the C-terminal segment. The C-terminal basic residues Lys62 and His64 together with Lys8 in the turn, which are critical for the bioactivities, may directly interact with the receptor site on the sodium channel. Residues Asn11 and Arg58, indispensable for the activities, are mainly responsible for stabilizing the distinct conformation of the putative bioactive site. Among others, His10 and His64 seem to be involved in the preference of BmK M1 for phylogenetically distinct target sites. The comparison of BmK M1 with Aah2 (classical α-toxin) and LqhαIT (α-insect toxin) showed that the specific orientation of the C-terminus mediated by the reverse turn might be relevant to the preference of α-toxin subgroups for phylogenetically distinct yet closely related receptor sites. The Y5G mutation indicated the "conserved hydrophobic surface" might be structurally important for stabilizing the *β*-sheet in the α/*β*-scaffold. The observations in this work shed light on the nature and roles of the residues possibly involved in the biological activity of a scorpion α-like toxin.

Voltage-gated sodium channels are transmembrane proteins responsible for the rising phase of action potentials in most excitable cells. They can be rapidly activated and inactivated upon depolarization of the cell membrane, which results in a transient and selective increase in Na^+ conductance. The central, pore-forming α-subunit of Na^+ channels has four homologous domains (I−IV), each with six α-helical transmembrane segments (S1−S6) (*1*). Being critical elements in excitability, Na^+ channels are the target of several kinds of neurotoxins, including scorpion neurotoxins (*2*). As a consequence, these toxins are essential tools for investigating the tissue distribution and functional properties of Na^+ channels. The scorpion toxins active on Na^+ channels have been divided into two major classes, α- and *β*-toxins. Scorpion α-neurotoxins, the most extensively studied group of scorpion toxins, are single-chain peptides composed of 60−70 amino acids cross-linked by four disulfide bonds. They prolong the action potential by slowing the inactivation of Na^+ currents with no direct effect on activation (*3*−*5*). The binding site of α-neurotoxins, so-called receptor site 3, has been located at the extracellular loop between segments S3 and S4, in the fourth domain of the α-subunit (IVS3−IVS4) (*6*). It seems that α-toxins act by preventing the outward movement of the IVS4 segment that is necessary for the rapid inactivation of the channel (*7*).

The scorpion α-neurotoxins can be further divided into three pharmacological subgroups according to their preferential toxicity to mammals or insects (*8*). The classical α-toxins or anti-mammal toxins (e.g., Aah2 or Lqh2) are highly toxic to mammals and weakly active on insects, whereas the anti-insect α-toxins (e.g., LqhαIT) are highly toxic to insects but poorly active on mammals when tested by intracerebroventricular (icv) injection at least. The α-like toxins (e.g., Lqh3), characterized more recently, act on both insects and mammals but are unique in their inability to bind to rat brain synaptosomes despite a high toxicity by icv injection (*9*). To understand the molecular mechanism of their

† This work was supported by the National Natural Science Foundation of China (Grants 30170210 and 39970158) and the Ministry of Science and Technology (Grant G19990756 and Grant G1988051100).

* To whom correspondence should be addressed. C.-W.C.: telephone, 86-21-54921165; fax, 86-21-54921011; e-mail, chi@sunm.shcnc.ac.cn. D.-C.W.: telephone, 86-10-64888547; fax, 86-10-64888560; e-mail, dcwang@sun5.ibp.ac.cn.

‡ Shanghai Institute of Biochemistry and Cell Biology, Chinese Academy of Sciences.

§ Institute of Biophysics, Chinese Academy of Sciences.

∥ CEA.

⊥ University of Angers.

@ N. Copernicus University.

10.1021/bi0270438 CCC: $25.00
Published on Web 04/02/2003

A

turn C-terminus

10 20 30 40 50 60

classical α toxins:

```
Aah2     VKDGYIVDDVNCTYFCGR-NAYCNEECTKLKGESGYCQWASPYGNACYCYKLPDHVRTKGPG-RCH(NH2)
BmK M8   GRDAYIADSENCTYFCGS-NPYCNDVCTENGAKSGYCQWAGRYGNACYCIDLPASERIKEGG-RCG
Lqh2     IKDGYIVDDVNCTYFCGR-NAYCNEECTKLKGESGYCQWASPYGNACYCYKLPDHVRTKGPG-RCR(NH2)
Lqq5     LKDGYIVDDKNCTFFCGR-NAYCNDECKKKGGESGYCQWASPYGNACWCYKLPDRVSIKEKG-RCN(NH2)
```

α-like toxins:

```
BmK M1   VRDAYIAKPHNCVYECAR-NEYCNDLCTKNGAKSGYCQWVGKYGNGCWCIELPDNVPIRVPG-KCH
BmK M4   VRDAYIAKPENCVYHCAG-NEGCNKLCTDNGAESGYCQWGGRYGNACWCIKLPDDVPIRVPG-KCH
Bom3     GRDGYIAQPENCVYHCFPGSSGCDTLCKEKGATSGHCGFLPGSGVACWCDNLPNKVPIVVGGEKCH
Bom4     GRDAYIAQPENCVYECAK-NSYCNDLCTKNGAKSGYCQWLGKYGNACWCEDLPDNVPIRIPG-KCHF
Lqh3     VRDGYIAQPENCVYHCFPGSSGCDTLCKEKGGTSGHCGFKVGHGLACWCNALPDNVGIIVEGEKCHS(NH2)
Lqh6     VRDGYIAQPENCVYHCIP---DCDTLCKDNGGTGGHCGFKLGHGIACWCNALPDNVGIIVDGVKCHK(NH2)
Lqh7     VRDGYIAKPENCAHHCFPGSSGCDTLCKENGGTGGHCGFKVGHGTACWCNALPDKVGIIVDGVKCH
```

α-insect toxins:

```
Lqq3     VRDAYIAKNYNCVYECFR-DSYCNDLCTKNGASSGYCQWAGKYGNACWCYALPDNVPIRVPG-KCH
LqhαIT   VRDAYIAKNYNCVYECFR-DAYCNELCTKNGASSGYCQWAGKYGNACWCYALPDNVPIRVPG-KCR
```

B

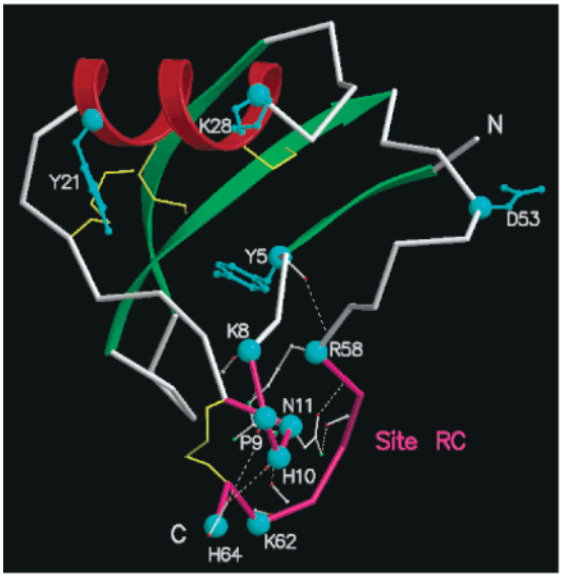

FIGURE 1: Location of the residues selected for mutagenesis on the sequence (A) and 3D structure (B) of BmK M1. (A) Comparison of the amino acid sequences of different subgroups of scorpion α-toxins. Sequences are aligned with cysteine frame, and deletions are introduced for maximum accuracy. The positions are numbered in terms of BmK M1. The residues mutated in this work are indicated in gray. Aah2 is from the scorpion *Androctonus australis* Hector (*42*). BmK M1, M4, and M8 are from *B. martensi* Karsch (*12*, *13*, *43*). Lqh2, Lqh3, Lqh6, Lqh7, and LqhαIT are from *L. quinquestriatus hebraeus* (*24*, *25*, *44*). Lqq3 and Lqq5 are from *Leiurus quinquestriatus quinquestriatus* (*45*, *46*). Bom3 and Bom4 are from *Buthus occitanus mardochei* (*28*). (B) Selected mutation sites in relation to the reverse turn 8−12 and C-terminal segment 58−64 are indicated with cyan-colored α-carbon atoms. The mutation sites in the conserved hydrophobic surface (CHS) (Y5), near the N-terminus (D53), and opposite the CHS (Y21 and K28) are shown with their side chains.

phylogenic selectivity, we need to identify the residues involved in receptor binding and the relevant structural elements for the functional sites of scorpion toxins. To date, for α-toxins, the mutagenesis approach has been successfully used in only one anti-insect α-toxin, LqhαIT (*10*). On the basis of an efficient yeast expression system for the α-like toxin BmK M1, found in our laboratory (*11*), the possible functionally important residues of this toxin were also investigated by site-directed mutagenesis.

BmK M1 is a representative neurotoxin from the scorpion *Buthus martensi* Karsch (BmK), and considered an α-like toxin according to sequence homology (Figure 1A) (*12*). Compared with structures of the classical α-toxins, BmK M8 (*13*) and Aah2 (*14*), the crystal structure of BmK M1 at high resolution (*12*) revealed some striking features despite the highly similar scaffold. First, a non-proline *cis* peptide bond between residues 9 and 10 unusually occurs in the five-residue reverse turn 8−12. Second, the *cis* peptide 9−10 mediates the spatial relationship between this turn and the C-terminal stretch through a pair of hydrogen bonds between residues 10 and 64 to make the orientation of C-terminal residues 62−64 distinct from the classical α-toxins (Figure 1B). In fact, the five-residue reverse turn 8−12 and the C-terminal segment 58−64 are closely connected by the fourth disulfide bond (12−63) and a hydrogen bond network to form a unique tertiary arrangement which was designated as site RC (*12*). In light of these comparisons, our mutagenesis analyses were concentrated on the significant residues

involved in this site, including residues 8−11, 58, 62, and 64. Some residues at locations putatively significant, including residue 5 on the "conserved hydrophobic surface" (CHS),[1] residue 53 near the N-terminus, and residues 21 and 28 on face B (*13*) opposite CHS, were also selected for mutation (Figure 1B).

With the efficient yeast expression system (*11*), BmK M1 and its 14 mutants were expressed and then investigated in terms of toxicity to mice, binding to insect and rat brain synaptosomes, and electrophysiological effects on Na^+ currents. In addition to pharmacological identification of BmK M1 as an α-like toxin, the results indicating a possible functional site and certain structural elements probably involved in phylogenetic specificity are reported.

MATERIALS AND METHODS

Materials. Escherichia coli strain DH5α was used for production of plasmids. Yeast strain *Saccharomyces cerevisiae* S-78 (Leu2, Ura3, Rep4) and expression vector pVT102U/α were used for expression of wild-type and mutated BmK M1. Chromatography media were from Pharmacia and trifluoroacetic acid and acetonitrile for high-performance liquid chromatography (HPLC) from Merck. The toxins Lqh3 (LTX002) and Lqh2 from the *Leiurus quinquestriatus hebraeus* scorpion were from Latoxan (Rosans, France) and in part were a generous gift from P. Sautière (Institute Pasteur, Lille, France). The reverse-phase C18 (250 mm × 4.6 mm; 30 nm, 5 μm particle size) HPLC column was from Vydac (Mojave, CA). Iodogen was from Pierce Chemicals (Rockford, IL) and carrier-free $Na^{125}I$ from Amersham (Buckinghamshire, United Kingdom). All other chemicals were of analytical grade. Filters for binding assays were glass fiber GF/C filters (Whatman, Maidstone, United Kingdom) preincubated in 0.3% polyethylenimine (Sigma, Steinhem, Germany).

Mutation, Expression, and Purification of BmK M1. On the basis of a comparison of the sequence and crystal structure of BmK M1 with those of other α-toxins (Figure 1), site-directed mutations were designed and introduced by polymerase chain reaction (PCR) with corresponding synthetic primers (*15*, *16*). Then the mutated cDNA was inserted into the yeast expression vector pVT102U/α and expressed in *S. cerevisiae* S-78 as previously described (*11*). Following centrifugation of the culture medium, the recombinant toxins were purified to homogeneity by ion-exchange chromatography and HPLC (*16*). Finally, the expressed samples were examined by mass spectrometry to confirm the mutation and purity. Recombinant products ranging from 1 to 12 mg could be purified from 1 L of culture medium. For most mutant toxins, the yield exceeded 5 mg/L, but for the Y5G mutant, it was only ∼1 mg/L.

Toxicity Assay. The fifty percent lethal doses (LD_{50}) of wild-type BmK M1 and its mutants were determined according to the method of J. Meier (*17*). Different amounts of toxins were dissolved in 0.9% NaCl and injected into the tail vein of KunMing male mice (20 ± 2 g). Paralysis of the rear legs, loss of balance, respiratory abnormality, incontinence, and eventually death were the successive symptoms induced by the toxins on mice. The body weight, injection dose, and survival time were recorded for calculation of the LD_{50}.

The toxicity of the BmK M1 mutants on the central nervous system of Swiss Webster mice (20−22 g) was measured by intracerebroventricular (icv) injection using a stereotaxic micromanipulator (Harvard/ASI Apparatus, Kent, England). After 200 pmol of different mutants had been injected, rapid running and jumping appeared prior to death. The time of appearance of the rapid running symptom was recorded.

Circular Dichroism Measurement. The protein samples used for circular dichroism (CD) spectrum analyses were dissolved in 25 mM Tris-HCl (pH 8.0) at a concentration of 200 μg/mL. Spectra were measured at room temperature in a 1 mm path length cuvette from 250 to 190 nm with a JASCO (Tokyo, Japan) J-715 spectropolarimeter. Data were collected at 0.1 nm intervals with a scan rate of 10 nm/min.

Neuronal Membrane Preparation. All buffers contained a cocktail of protease inhibitors composed of phenylmethanesulfonyl fluoride (50 μg/mL), pepstatin A (1 μM), iodoacetamide (1 mM), and 1 mM 1,10-phenanthroline. According to the methods of Kanner (*18*) and Gilles et al. (*19*), rat brain synaptosomes were prepared from adult albino Sprague-Dawley rats (∼300 g, laboratory-bred). Insect synaptosomes were prepared from whole heads of adult *Periplaneta americana* cockroaches according to the method of Krimm et al. (*20*). The membranes were kept at −80 °C until they were used. No loss of binding activity was observed after at least 6 months. The membrane protein concentration was determined using a Bio-Rad protein assay, using bovine serum albumin (BSA) as a standard.

Radioiodination. Lqh2, Lqh3, and Bj-xtrIT were radioiodinated with Iodogen using 5 mg of toxin and 0.5 mCi of carrier-free $Na^{125}I$, as described for LqhαIT (*9*, *21*). The monoiodotoxins were purified with a Vydac RP C18 column using a gradient of acetonitrile from 0 to 45% B in 5 min, and then to 80% B in 105 min, to ensure the best separation of iodinated products (A being aqueous 0.1% TFA and B being 0.085% TFA and 50% acetonitrile) at a flow rate of 1 mL/min. The single radioactive peak of ^{125}I-labeled toxins was eluted after the unlabeled toxin at 27 and 33% acetonitrile for the Lqh toxins and Bj-xtrIT, respectively. The yield of iodination was less than 5%. The concentration of the radiolabeled toxin was determined according to the specific activity of ^{125}I corresponding to 2500−3000 dpm/fmol of monoiodotoxin, depending on the age of the radiotoxin and by estimation of its biological activity (usually 50−80%). The biological activity of a labeled toxin was determined from the ratio of bound toxin (total binding) at a constant, low concentration of labeled toxin to the total radioactive toxin present in the reaction. The measurements were performed at increasing concentrations of receptors (membranes). Were the biological activity of the radioiodinated toxin to be 100%, all labeled ligand should be bound at a saturating receptor concentration. However, since radioiodination is always associated with some irreversible loss of toxin activity, the percent of bound toxin at a saturating receptor concentration represents the biological activity of the labeled toxin.

[1] Abbreviations: HPLC, high-performance liquid chromatography; LD_{50}, 50% lethal dose; CD, circular dichroism; TTX, tetradotoxin; AP, action potential; HP, holding potential; CHS, conserved hydrophobic surface.

Binding Assay. The standard binding medium consisted of 130 mM choline chloride, 1.8 mM $CaCl_2$, 5.5 mM KCl, 0.8 mM $MgSO_4$, 50 mM HEPES, 10 mM glucose, and 2 mg/mL BSA. The wash buffer consisted of 140 mM choline chloride, 1.8 mM $CaCl_2$, 5.4 mM KCl, 0.8 mM $MgSO_4$, 50 mM HEPES, and 5 mg/mL BSA (pH 7.4). Rat brain or cockroach synaptosomes were suspended in 0.2 mL of binding buffer, containing ^{125}I-labeled toxins. After incubation, the reaction was terminated according to the method of Gilles et al. (*21*). The extent of nonspecific toxin binding was determined in the presence of an excess of unlabeled toxin. The equilibrium competition assay was performed using increasing concentrations of the unlabeled toxin in the presence of a constant low concentration of the radioactive toxin. Competition binding experiments were analyzed by the computer program KaleidaGraph (Synergy Software, Reading, PA) using a nonlinear Hill equation (for IC_{50} determination), and the K_i values were calculated by the equation $K_i = IC_{50}/(1 + L^*/K_d)$, where L^* is the concentration of the hot ligand and K_d is its dissociation constant (*22*).

Electrophysiology. Wild-type BmK M1 and two variants (Y5G and P9S) were tested at micromolar concentrations on the giant axons isolated from the nerve cord of the cockroach *P. americana*, using a double oil-gap technique, in both current-clamp and voltage-clamp configurations (*23*). The toxins were also tested on rat brain and skeletal muscle Na^+ channels ($rNa_v1.2A$ and $rNa_v1.4$, respectively) expressed in *Xenopus* oocytes, using a two-electrode voltage-clamp technique (*24*).

RESULTS

Biological Activity of BmK M1 on Insects. To identify the receptor site that is targeted by BmK M1 on insect Na^+ channels, the binding of radiolabeled toxins Lqh3 (*25*) and Bj-xtrIT (*26*), representing α- and β-classes, respectively, to cockroach synaptosomes was studied in the presence of increasing concentrations of BmK M1. The binding of the α-like toxin [^{125}I]Lqh3 (site 3) was fully inhibited by BmK M1 at low concentrations with a K_i value of 13.8 ± 0.8 nM (average of three experiments, Figure 2 and Table 1). On the other hand, BmK M1 did not displace the binding of [^{125}I]Bj-xtrIT (site 4) even at 10 μM (not illustrated).

The functional consequences of the binding of BmK M1 to insect neuronal membranes were assessed on isolated cockroach axons by electrophysiological methods. On this preparation, BmK M1 (1 μM) prolonged the falling phase of the evoked action potential (AP) in less than 3 min, while the resting potential and the AP amplitude were not modified (Figure 3A). After 3−4 min, "plateau" APs of more than 300 ms were recorded (Figure 3B). The plateau was followed by a long postdepolarization, so it was necessary to stimulate only at 30 or even 60 s intervals to avoid a summation of the postdepolarizations. In voltage-clamp experiments, application of long (300 ms) voltage pulses to −10 mV from a HP of −60 mV revealed that BmK M1 slows the Na^+ inactivation mechanism: 300 ms after the peak current, ~33% of I_{Na^+} persisted. At the end of the voltage pulse, deactivation was fast: the small inward tail current may be attributed to some local accumulation of Na^+ ions after a long pulse (Figure 3C). Postsuperfusion of the axon with 0.5 μM tetrodotoxin suppressed the peak and maintained currents, indicating that the modified currents were indeed passing through TTX-sensitive Na^+ channels (Figure 3D).

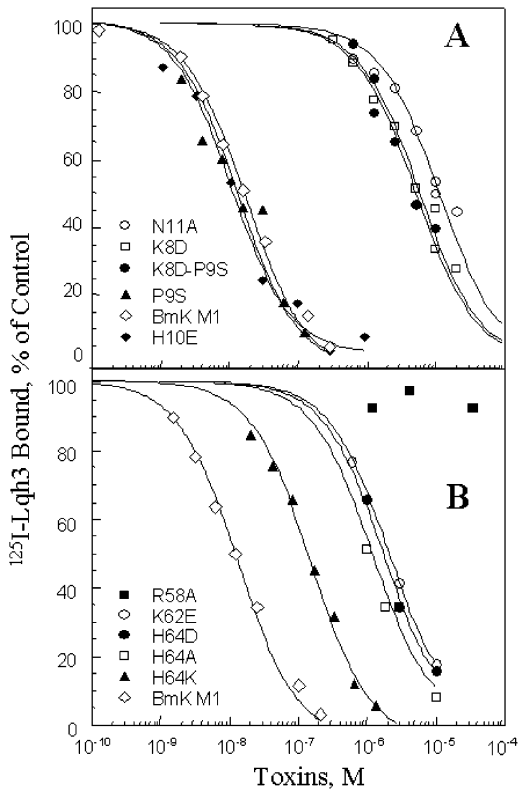

FIGURE 2: Competitive inhibition of [^{125}I]Lqh3 binding by different BmK M1 variants. Cockroach neuronal membranes (in 200 μL of binding buffer) were incubated with 250 pM [^{125}I]Lqh3 (K_d = 1.24 nM) (*21*) in the presence of increasing concentrations of recombinant BmK M1 variants. The level of nonspecific binding determined in the presence of 1 μM Lqh3 was subtracted. The inhibition of specific [^{125}I]Lqh3 binding is presented as a percentage of the control in the absence of unlabeled toxins. The data points were fitted with the nonlinear Hill equation.

Biological Activity of BmK M1 on Mammals. Following icv injection, BmK M1 killed mice with an LD_{50} of 38 pmol/mouse, thus showing a 5−10-fold lower toxicity than other α-like toxins such as Lqh3, Bom3, and Bom4 (*9*, *25*). Despite its toxicity in the brain, BmK M1 was unable to inhibit the high-affinity binding of the classical α-toxin Lqh2 on rat brain synaptosomes even at 60 μM. This striking discrepancy between the high toxicity in whole brain and the inability to bind to synaptosomes is in agreement with previous data obtained with other α-like toxins (*19*, *24*, *27*−*29*) and therefore represents one of the major features of this subgroup of scorpion α-toxins.

The first electrophysiological characterization of BmK M1 on a defined Na^+ channel subtype has recently shown a clear activity on cardiac Na^+ channels ($hNa_v1.5$ or hH1) expressed in *Xenopus* oocytes (*5*). Using the same expression system, we have examined whether BmK M1 also affects two other important Na^+ channel subtypes, $rNa_v1.2A$ (rat brain IIA) and $rNa_v1.4$ (rat skeletal muscle). The $rNa_v1.2A$ currents evoked by voltage pulses from −100 to −10 mV were not modified in the presence of the toxin for 15 min even at 10 μM (Figure 4A). This lack of an effect was further demonstrated using a wide range of test potentials, as shown by the current−voltage curves of Figure 4B. In contrast, 1 μM BmK M1 increased the peak current amplitude of

Table 1: Activity of BmK M1 and Its Mutants on Insect and Mouse Channels

	insect		mammal			
	neuronal membranes of *P. americana*		peripheral nervous and muscular systems		central nervous system	
	K_i[a] (nM)	increase in K_i (fold)	LD_{50}[b] (mg/kg)	increase in LD_{50} (fold)	running time[c] (min)	increase in time (min)
wild type	13.8 ± 0.8 (n = 3)	1	0.53 ± 0.064	1	4 ± 2	1
Y5G	989 ± 114 (n = 2)	70	/[d]	∞		
K8D	3500 ± 250 (n = 2)	250	62.60 ± 0.73	118	50 ± 10	12
K8D/P9S	2295 ± 220 (n = 2)	170	22.98 ± 7.17	43.4	51 ± 10	12
P9S	17.8 ± 3.8 (n = 2)	1.3	0.95 ± 0.012	1.8	4.5 ± 0.5	1
H10E	10.9 ± 1.5 (n = 3)	0.8	0.91 ± 0.034	1.7	11 ± 3	3
N11A	5260 ± 130 (n = 2)	380	/[d]	∞	50 ± 25	12
Y21G	19.1 ± 8.9 (n = 2)	1.4	1.01 ± 0.055	1.9	6 ± 1	1.5
K28E	195 ± 4 (n = 2)	14	2.20 ± 0.049	4.1		
D53A	2.57 ± 0.5 (n = 2)	0.2	0.33 ± 0.047	0.6		
R58A	≫20000 (n = 2)	>1600	/[d]	∞		
K62E	2309 ± 168 (n = 2)	170	37.87 ± 3.12	71.4	>120	>60
H64D	2450 ± 700 (n = 2)	180	23.28 ± 2.84	43.9		
H64A	1330 ± 110 (n = 2)	96	2.01 ± 0.096	3.8	10 ± 3	2.5
H64K	158 ± 10 (n = 2)	11.5	1.00 ± 0.031	1.9	10 ± 2	2.5

[a] K_i was determined on synaptosomes from the cockroach *P. americana*. [b] LD_{50} was determined by tail vein injection into mice. [c] Running time was determined by icv injection into mice (200 pmol/mouse). [d] The toxicity of Y5G, N11A, and R58A was not detectable since 2 mg of toxin induced no symptom in a mouse.

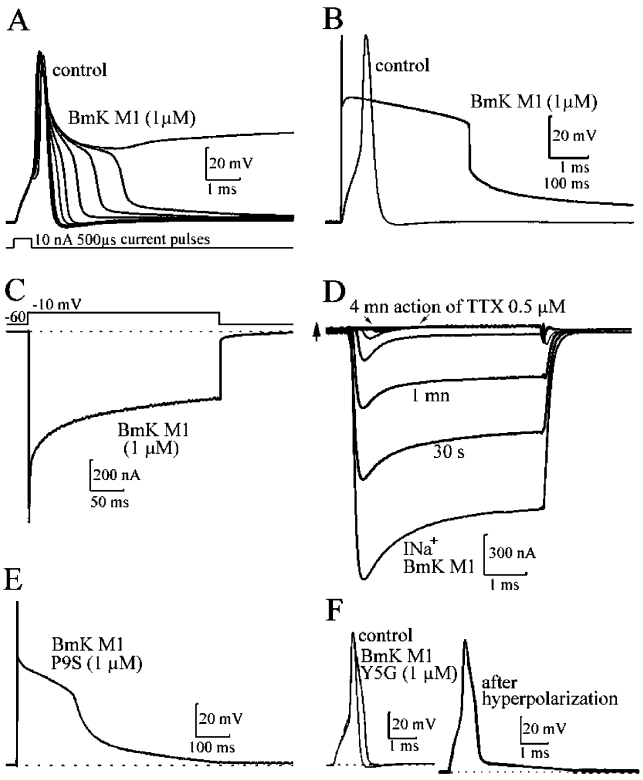

FIGURE 3: Actions of BmK M1, mutant P9S, and mutant Y5G on the cockroach isolated axon. Prolongation of evoked action potentials, resulting in "plateau" potentials, was obtained with BmK M1 (A and B) as well as with the P9S mutant (E), but not with the Y5G mutant (F). Such plateau potentials are due to the slowing of Na^+ current inactivation (C) in TTX-sensitive voltage-gated Na^+ channels (D).

$rNa_v1.4$ currents and modified the kinetics of their decaying phase (Figure 4C, left traces). Inactivation of $rNa_v1.4$ currents was best fitted by the sum of two exponentials, both in the control and in the presence of BmK M1. The fast inactivation time constant ($\tau_1 \sim 2.7$ ms) was not consistently modified by the toxin, whereas the slow component time constant (τ_2) was increased by ~3-fold (Figure 4D). BmK M1 (1 μM) also induced a negative shift of the left part of I/V curves (5.3 ± 0.6 mV at midactivation, n = 4), indicating channel openings at more hyperpolarized potentials than in controls (Figure 4E).

All these data demonstrated clearly that BmK M1 is an α-like toxin, as previously suggested by sequence comparison.

Mutations in the Five-Residue Reverse Turn. The five-residue reverse turn 8−12 contains two residues, Asn11 and Cys12, that are conserved in all α-toxins, while the three others, residues 8−10, form a molecular signature typical of each of the three subgroups of α-toxins (Figure 1A). In the three-dimensional (3D) structure of α-like toxins, an unusual non-proline *cis* peptide bond has been found between Pro9 and His/Glu10 (*12*, *30*; PDB entries 1FH3 and 1BMR). Mutation of these two residues (P9S and H10E) barely affected the activity on insect and mammal Na^+ channels (Table 1 and Figures 3E and 4C), while the residues before and after the *cis* peptide bond were more influential. Replacement of Lys8 with Asp, the corresponding residue in classical α-toxins, caused a 250-fold decrease in the binding affinity for insect Na^+ channels, while the toxicity to mice was decreased by 118-fold following tail vein injection and by 12-fold following icv injection (Table 1). Introduction of the P9S mutation into the K8D mutant (K8D/P9S double mutation) partially restored the biological activity. Another mutant, N11A, was almost not toxic to mice by tail vein injection even at a high concentration (2 mg/mouse), and it also showed a dramatic decrease in affinity for the cockroach Na^+ channel (380-fold) and toxicity to mouse brain (12-fold). The severe change in the CD spectrum implies that a structural destabilization should be the primary cause for the loss of toxicity (Figure 5A).

Mutations in the C-Terminal Segment. As the basic residues of the C-terminal segment have been shown to be important for the activity of LqhαIT and Aah2 (*10*, *31*), much attention was focused on this area. Arg58 seems to be the most crucial residue in the C-terminal segment since the R58A mutant was quite unable to recognize any of the insect

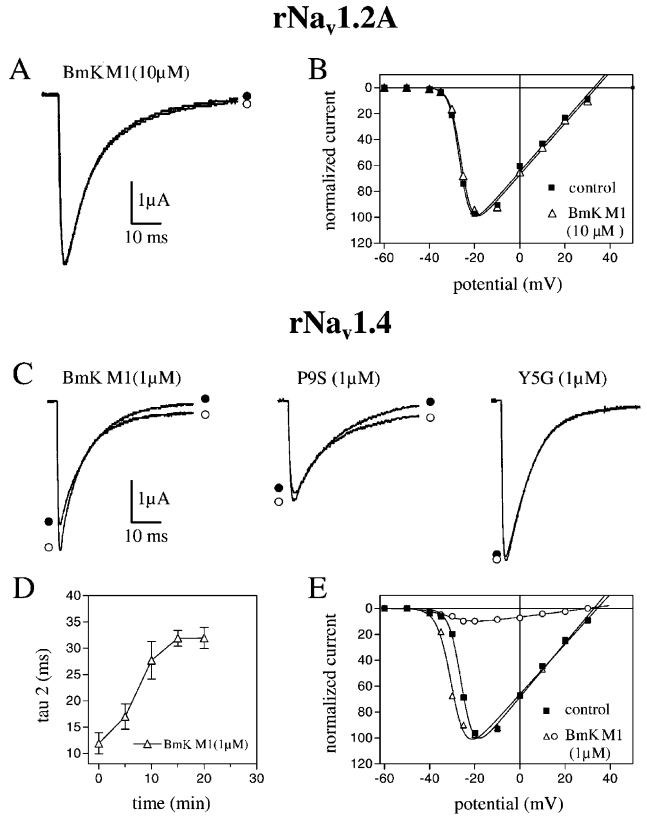

FIGURE 4: Effects of wild-type and mutant BmK M1 on Na^+ currents recorded from *Xenopus* oocytes expressing rat brain (rNa$_v$1.2A) or rat skeletal muscle (rNa$_v$1.4) voltage-gated Na^+ channels. (A and C) Current traces evoked by step depolarizations from −100 to −10 mV, before (●) and after (○) toxin application for 15 min. (B and E) Normalized current−voltage curves in control (■) and after equilibration with 1 μM BmK M1 [(△) peak currents and (○) late currents measured at the end of 50 ms pulses]. (D) Modification of the slow inactivation time constant (τ_2) of Na$_v$1.4 currents by 1 μM BmK M1. The toxin was applied at time zero.

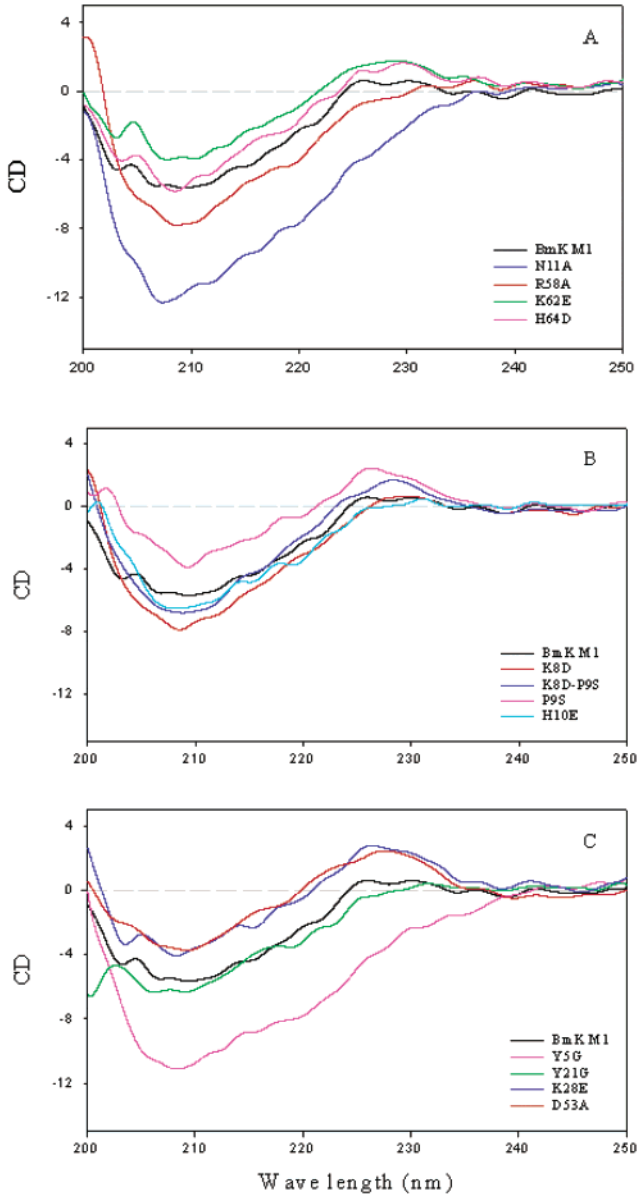

FIGURE 5: Circular dichroism spectra of BmK M1 and its mutants. BmK M1 is compared with mutants modified at the C-terminal region or at Asn11 (A), mutants modified around the *cis* peptide bond (B), and mutants modified at other sites (C). The spectra of H64A and H64K mutants, which remained similar to that of the unmodified toxin, were omitted.

or mammalian Na^+ channels targeted by BmK M1 (Table 1 and Figure 2B). This dramatic loss of activity pinpoints a "hot spot" residue, i.e., a residue that is indispensable for activity on both insect and mammal Na^+ channels.

Position 62 is occupied by a positively charged residue in all α-group toxins. Inversion of the charge of this residue (K62E mutation) remarkably decreased the apparent binding affinity for insect Na^+ channels (170-fold) and the toxicity to mammals via muscle and brain Na^+ channels (more than 70- and 60-fold, respectively). This implies that the positive charge of Lys62 strongly influences the affinity of BmK M1 for all the channels that were tested.

Within the α-like toxin group, the residue at position 64 is often a histidine. Replacement of this residue with alanine decreased the binding affinity of BmK M1 for the insect receptor site by 96-fold, whereas the toxic effects on mammals via binding to muscular and brain Na^+ channels were only mildly inhibited (3.8- and 2.5-fold, respectively). Replacement of Ala with the negatively charged Asp further decreased the binding affinity for insect Na^+ channels and the toxicity to mice. Of the three BmK M1 variants modified at position 64, H64K retained the highest activity; its level of binding to insect channels was much less reduced than for the two other variants, and its anti-mammal toxicity was almost the same as that for wild-type BmK M1 (Table 1), indicating clearly that the positive charge of residue 64 is beneficial to the binding and activity of this α-like toxin.

Mutations in the Conserved Hydrophobic Surface. A conserved aromatic cluster, also designated face A (*12*), exists in all the long chain scorpion toxins specific to voltage-gated Na^+ channels, including the α- and β-classes (*12*, *32*, *33*). Tyr5, the most conserved residue in this surface, was mutated to glycine (Y5G). This caused a remarkable change in the CD spectrum (Figure 5C), decreased the affinity of the toxin for insect Na^+ channels by a factor of 70, and abolished the lethality to mice even at a very high dose (2 mg/mouse) (Table 1). Accordingly, on the cockroach axonal preparation, external application of 1 μM Y5G for 5 min produced only a "shoulder" on the decaying phase of the evoked AP (Figure 3F). Artificial hyperpolarization, passing of a constant current through the axonal membrane, resulted

in a slight prolongation of the AP, but no plateau action potential could be evoked. As shown by Figure 4C (right record), 1 μM Y5G also did not appreciably modify the inactivation kinetics of Na^+ currents in oocytes expressing rat $Na_v1.4$ channels.

Some residues surrounding the conserved hydrophobic surface are also considered important. The negatively charged Asp53, which is close to this surface and also to the N-terminal residues, is highly conserved in different subgroups of α-toxins, while it is replaced with a neutral residue (Ala) in BmK M8 (Figure 1A). To test the implication of this substitution, the BmK M1 D53A variant was generated. Interestingly, this mutation increased the toxicity to mice by tail vein injection (60%) and the binding affinity for insect Na^+ channels (5-fold) (Table 1).

Mutations in Face B. The conserved residues Tyr21 and Lys28 are situated at the molecular surface, called face B, that is roughly opposite the conserved hydrophobic surface. They are included in the α-helix (residues 19−28) (Figure 1B). Replacement of Tyr21 with a Gly induced no significant change in the binding affinity for insect Na^+ channels, but the toxic effect on muscle Na^+ channels was slightly reduced (∼2-fold) (Table 1). On the other hand, the K28E mutation decreased the level of binding to insect channels (14-fold) and the toxicity to mice via muscle channels (4.1-fold) (Table 1). These meant that both the charge and hydrophobicity of face B might influence the binding and toxicity of BmK M1 to some extent.

DISCUSSION

During the two past decades, many efforts have been made to explore the functional site of scorpion toxins by different approaches (*31*, *34*, *35*), but it is only recently that the site-directed mutagenesis approach has become possible, based on the availability of efficient recombinant expression systems (*10*, *16*, *26*). BmK M1 is the first α-like toxin available in a recombinant form. In combination with its 3D structure determined by X-ray analysis, the site-directed mutagenesis of BmK M1 made possible a more direct investigation of the nature and roles of the residues involved in the bioactivity of this α-like toxin.

Pharmacological Identification of BmK M1 as an α-like Toxin. Though some initial bioassays and electrophysiological analysis were reported (*5*, *11*), the pharmacological properties of BmK M1 had not been thoroughly investigated. Because of the availability of recombinant BmK M1, a detailed study of its activity on different targets was undertaken in the work presented here. BmK M1 exhibits typical α electrophysiological effects, prolonging the inactivation phase of both insect and mammal Na^+ currents (Figures 3A and 4C). Similarly, its ability to inhibit the binding of α-toxins but not that of β-toxins on insect Na^+ channels (Figure 2A) also identifies BmK M1 as an α-toxin. Furthermore, its activity on both insect and mammal Na^+ channels and its inability to bind to $rNa_v1.2A$ (Figure 4A) and synaptosomal Na^+ channels in rat brain demonstrate unambiguously that BmK M1 is a typical α-like toxin, as suggested previously by sequence comparison (*12*).

A Putative Functional Site. The X-ray crystal structure showed a peculiar site formed by the five-residue reverse turn 8−12 and the C-terminal segment 58−64 protruding from the scaffold of BmK M1 (Figure 1B), which has been designated site RC previously (*12*). A total of 10 mutants in this area have been analyzed, including all residues in the turn except Cys12, and the most significant residues (58, 62, and 64) in the C-terminal segment (Figure 1B). The results (Table 1) showed that most residues in this site, including Lys8, Asn11, Arg58, Lys62, and His64, are crucial for the bioactivities of the toxin. These data, in association with the unique tertiary organization of site RC, provide an insight into the putative functional site of BmK M1 (Figure 6).

The residues that are important for bioactivity may play a role either in receptor site recognition or in the unique conformation of the toxin polypeptide. The C-terminal residues Lys62 and His64, together with the reverse turn residue Lys8, probably interact directly with the receptor site since their acidification (K8D, K62E, and H64D) dramatically decreased the toxicity to both mice and insects without marked changes in CD spectra. The importance of positive charges at the C-terminus was further documented by a series of mutations at residue 64 (H64D, H64A, and H64K). Some work on other similar toxins also showed that their toxicity could be increased when His64 was positively charged (*21*, *36*). Accordingly, in the mammal $Na_v1.4$ channels, an acidic residue of the IVS3−IVS4 loop is required for the binding of α-like scorpion toxins (*37*). Together, these data suggested that the positive residues of site RC interact electrostatically with the receptor site of Na^+ channels. Besides, the pK_a of histidine is believed to be between 6 and 7 (*21*, *36*). Therefore, at physiological pH (∼7.5), His64 should not be positively charged. However, the most favorable residue at this position was found to be His, as already observed for LqhαIT (*10*, *38*) and in this study. These arguments indicate that, in addition to the positive charge, the stereochemical specificity of this residue is also crucial for the binding and toxic activity.

Two other residues in the same area, Asn11 and Arg58, are mainly responsible for stabilizing the unique conformation of the functional site. Indeed, mutating either of these two residues severely reduced the bioactivity of the toxin (Table 1) while markedly altering its conformation, as inferred from changes in CD spectra (Figure 5A). Residue Asn11, which is strictly conserved in all α-toxins (Figure 1A), is buried in the native toxin and provides side chain atoms $O^{\delta1}$ and $N^{\delta2}$ to connect the main chain of Val59 through the $11O^{\delta1}\cdots N59$ and $11N^{\delta2}\cdots O59$ hydrogen bonds. Besides, the carbonyl oxygen of Asn11 makes a hydrogen bond with N^{ϵ} of Arg58, which further connects Gly61 and Tyr5 via a pair of hydrogen bonds (Figure 6B). Residue 58, which is conserved as Arg or Lys in most α-toxins, has been shown to be crucial for activity in different α-toxin subgroups (ref *31* and this study), although it is located in a rather inaccessible cavity. Its side chain is connected with the main chain of Asn11 and Gly61 (Figure 6B). Through these complicated interactions contributed by Asn11 and Arg58, in addition to the disulfide bond 12−63, the five-residue reverse turn 8−12 is closely correlated with the C-terminal segment 58−64 to form a local tertiary structure unique for this functional site. Obviously, the conformational change due to the loss of the side chains of Asn11 and Arg58 should be the reason for the extremely low activity of variants N11A and R58A.

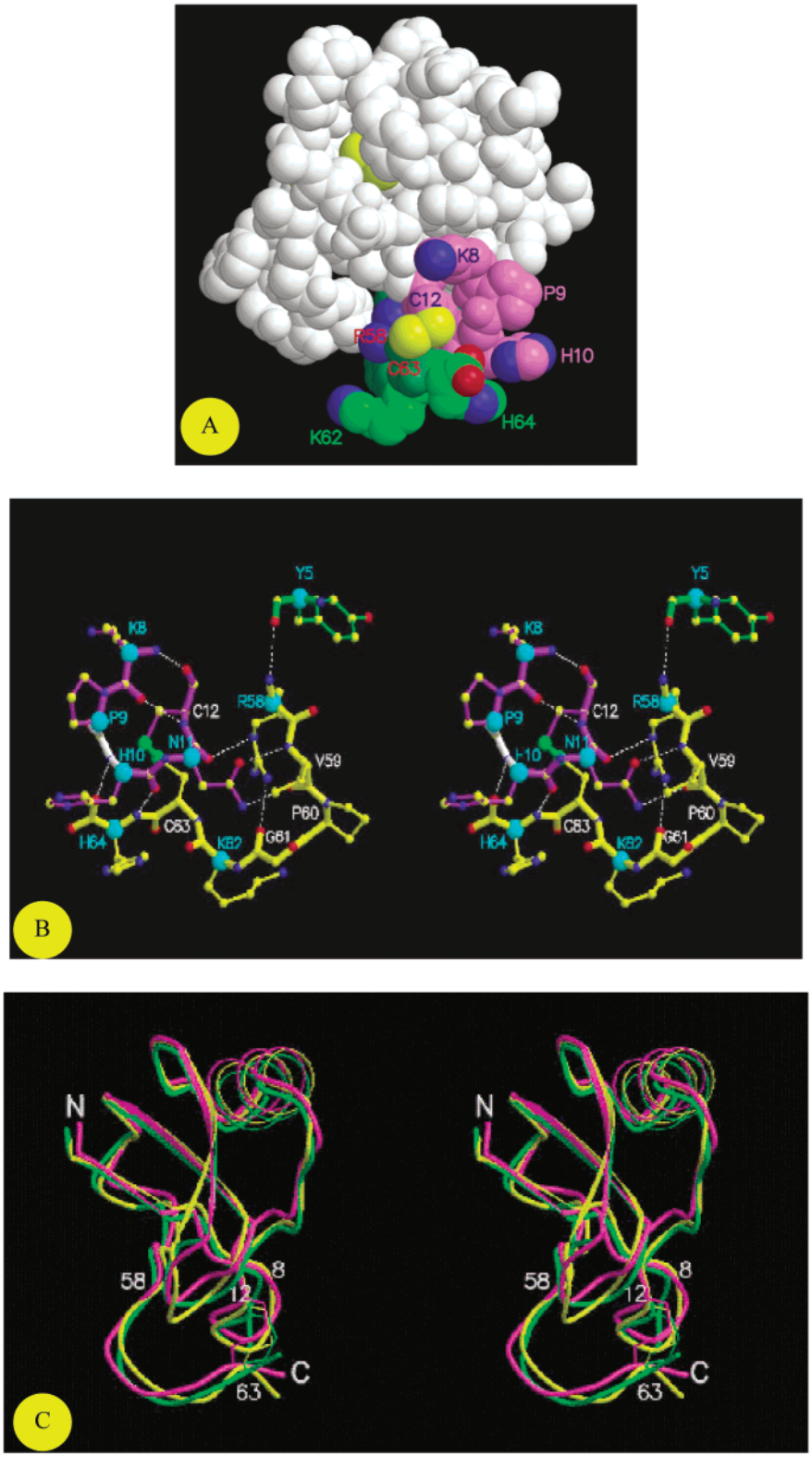

FIGURE 6: Putative functional site of BmK M1 and superposition of α-subgroup toxins. (A) The exterior of the functional site is colored green (C-terminal segment) and purple (reverse turn 8−12). On the space-filling model of BmK M1, C-terminal residues Lys62 and His64 together with Lys8 may be involved in toxin−receptor binding and His10 and His64 may relate to the interactions with phylogenetically distinct target sites. N, O, and S atoms are colored blue, red, and yellow, respectively. (B) Hydrogen bond network in the putative functional site. Among others, residues Asn11 and Arg58 provide complicated contacts between the C-terminal segment and the reverse turn 8−12 to stabilize the unique tertiary arrangement of the functional site. The disulfide bridge 12−63 and the *cis* peptide bond between residues 9 and 10 are highlighted with green and white, respectively. (C) Superposition of the α-carbon backbone of BmK M1 (yellow) with Aah2 (green) and Lqh αIT (magenta) showing the distinct orientations of the C-terminus in correlation with the reverse turn 8−12 and the disulfide bridge 12−63 in the α-toxin subgroups. This figure was prepared with MolScript (*47*) and rendered with Raster3D (*48*). All coordinates were taken from the Protein Data Bank.

Pro9 is conserved in all α-like toxins, but it is replaced with an Asp in most classical α-toxins (Figure 1A). The moderate effects of mutations P9S and H10E, in contrast with the significant effects of substitutions at the other residues of the reverse turn, indicated that residues 9 and 10 are not critical for bioactivity. However, the K8D/P9S double mutation partially restored the bioactivities in comparison with the variant K8D. The crystal structure of the mutant P9S, determined at a high resolution most recently, revealed that the peptide bond (9−10) is still in the *cis* form, but rather flexible with very high temperature factors (Y. Xiang, personal communication). These observations showed that the importance of Pro9, present as a conformationally confined residue, is mainly in stabilizing the unique *cis* peptide bond.

Possible Structural Elements Involved in the Preference for Distinct Targets. As indicated in the introductory section, α-toxins are divided into three distinct pharmacological subgroups according to their preference for mammal or insect target sites (*8*, *24*, *39*). The question of whether the main structural elements involved in this preference are included in the putative functional site deduced from mutagenesis analysis then arises.

The putative functional site is anchored to the molecular scaffold through the disulfide bridge 12−63 and is stabilized by a cooperative interaction between the reverse turn 8−12 and the C-terminal segment 58−64 (Figure 6A,B). By comparison of the 3D structure of Aah2, BmK M1, and Lqh αIT, representative toxins of the classical α-, α-like, and α-insect subgroups, respectively, it appears that the most striking differences occur at the C-terminus. In particular, the orientation of this stretch clearly differs in the three toxins, due to the variable conformation of the disulfide bridge 12−63 and reverse turn 8−12 (Figure 6C). This structural diversification within the functionally important site RC should have facilitated the adaptation of α-group toxins to phylogenetically distinct receptor sites on Na^+ channels during evolution (*40*).

In our mutagenesis analysis, most of the mutations similarly affected the anti-insect and anti-mammal activities of BmK M1 (Table 1), which implies a high level of conservation of receptor site 3 in phylogenetically distant Na^+ channels. However, two mutations in the putative functional site differentially modified the activity of BmK M1 on insect and mammal channels. The first one, the H10E mutation, did not significantly affect the binding of the toxin to insect Na^+ channels but decreased its anti-mammal activity (Table 1). Although the decrease was moderate, it appears that His at position 10 is more suitable than Glu for the activity of BmK M1 on mammal Na^+ channels. Another position deserving more attention is His64. Neutralization of this residue (H64A) severely decreased the binding affinity for cockroach Na^+ channels (96-fold), while toxicity to mice was mildly reduced (3.8-fold) (Table 1), thus showing that insect Na^+ channels are much more sensitive to a histidine at position 64 than mammal Na^+ channels. Accordingly, His64 is not strictly conserved in classical (anti-mammal) α-toxins (Figure 1A). Together, these results support the hypothesis that the putative functional site contains the structural elements relevant to the phylogenetic preference of α-toxin subgroups.

Roles of Residues in Other Areas. Residue Tyr5 is located in the center of a conserved aromatic cluster. The Y5G mutation caused a striking change in the CD spectrum as well as a dramatic decrease in toxicity to mouse and binding affinity for insect Na^+ channels (Table 1 and Figure 5C). It is most likely that removal of the central aromatic group of the hydrophobic surface destabilizes the overall folding of the toxin, eventually leading to a quasi-total loss of activity. The fairly low expression yield of this mutant may also be explained by the difficulty of folding.

Another mutation site (Asp53) is close to the N-terminus, notably to Arg2, a residue that has been reported to be significant for toxicity (*34*, *41*). The D53A mutation is the only one that increased the activity of the toxin. The same substitution in an acidic toxin, BmK M8, is known to mediate the translocation of the N-terminus and the side chain of Arg2 (*13*). Consequently, the α-amino group of the N-terminus changes to a new position, and the functional group of Arg2 protrudes from the molecular surface, instead of being buried as in Aah2 and BmK M1. It is therefore plausible that the translocation of Arg2 may facilitate a favorable electrostatic interaction with Na^+ channels. The D53A mutation may also contribute to this effect by making the electrostatic potential less negative.

Face B, the opposite surface of the conserved hydrophobic surface, has no clear structural boundary. No residue of this face has been found to be crucial for the activity of any group of α-toxins. In BmK M1, the inverse charge mutation K28E caused a moderate decrease in the effects on both mice and cockroaches. The effect of the Y21G mutation was even milder for both structure and activity (Table 1 and Figure 5C), although Gly is a gentle helix breaker. The weak effect of Y21G could be interpreted with a series of structural factors. First, Tyr21 is located at the beginning of the helix (residues 19−28). Second, Tyr21 is just neighboring a disulfide bridge, 24−46, between the α-helix and a β-strand (β3). Third, the side chain of Tyr21 is situated on the surface of face B without strong contacts with surrounding residues as shown in the crystal structure (*12*). These results suggest that face B does not play a major role in the interaction with the target.

In conclusion, by exploiting a multidisciplinary approach, we have elucidated the functional site of a representative α-like scorpion toxin for the first time. Most of the residues that are important for bioactivity are located in site RC, a unique tertiary arrangement that was previously resolved by X-ray crystallography. Within this site, the basic residues Lys62, His64, and Lys8 should bind directly to the receptor site of Na^+ channels through electrostatic interactions. Because of its functional importance, site RC exhibits a perfectly well organized structure that is maintained by residues such as Asn11 and Arg58 (Figure 6). The specific orientation of the C-terminus, mediated by the reverse turn 8−12, might be relevant to the preference of α-toxins for phylogenetically distinct receptor sites.

ACKNOWLEDGMENT

We thank Dr. YouShang Zhang (Shanghai Institute of Biochemistry) for the pVT102U/α vector, Dr. Peter Backx (University of Toronto, Toronto, ON) for the pGW1H/$rNa_v1.4$ construct, and Dr. Robert Dunn (McGill University,

Montreal, PQ) for the pHL/rNa$_v$1.2A construct. We also thank Dr. Dalia Gordon and Dr. Michael Gurevitz (Tel Aviv University, Tel Aviv, Israel) for having supplied Bj-xtrIT, and we appreciate Ye Xiang (Institute of Biophysics, Beijing, China) for his kind help in figure preparation.

SUPPORTING INFORMATION AVAILABLE

Figure 1 shows the competition of Lqh2 and BmK M1 for the binding of the classical α-toxin [^{125}I]Lqh2 in rat brain synaptosomes. Rat brain synaptosomes (17.5 μg of protein/mL) were incubated with 84 pM [^{125}I]Lqh2 for 20 min at 20 °C in the presence of increasing concentrations of Lqh2 or BmK M1. The level of nonspecific binding determined in the presence of 300 nM Lqh2 was subtracted. The inhibition of specific [^{125}I]Lqh2 binding is presented as a percentage of the control in the absence of unlabeled toxins. The data points were fitted with the nonlinear Hill equation. The calculated K_i of Lqh2 is 0.3 ± 0.1 nM (n = 3). Figure 2 shows the competitive inhibition of [^{125}I]Lqh3 binding by different BmK M1 variants. Cockroach neuronal membranes (in 200 μL of binding buffer) were incubated with 250 pM [^{125}I]Lqh3 (K_d = 1.24 nM) (*21*) in the presence of increasing concentrations of recombinant BmK M1 variants. The level of nonspecific binding determined in the presence of 1 μM Lqh3 was subtracted. The inhibition of specific [^{125}I]Lqh3 binding is presented as a percentage of the control in the absence of unlabeled toxins. The data points were fitted with the nonlinear Hill equation. This material is available free of charge via the Internet at http://pubs.acs.org.

REFERENCES

1. Catterall, W. A. (2000) *Neuron 26*, 13−25.
2. Cestèle, S., and Catterall, W. A. (2000) *Biochimie 82*, 883−892.
3. Couraud, F., Jover, E., Dubois, J. M., and Rochat, H. (1982) *Toxicon 20*, 9−16.
4. Possani, L. D., Becerril, B., Delepierre, M., and Tytgat, J. (1999) *Eur. J. Biochem. 264*, 287−300.
5. Goudet, C., Huys, I., Clynen, E., Schoofs, L., Wang, D. C., Waelkens, E., and Tytgat, J. (2001) *FEBS Lett. 495*, 61−65.
6. Rogers, J. C., Qu, Y., Tanada, T. N., Scheuer, T., and Catterall, W. A. (1996) *J. Biol. Chem. 271*, 15950−15962.
7. Sheets, M. F., Kylem, J. W., Kallen, R. G., and Hanck, D. A. (1999) *Biophys. J. 77*, 747−757.
8. Gordon, D., Savarin, P., Gurevitz, M., and Zinn-Justin, S. (1998) *J. Toxicol., Toxin Rev. 17*, 131−159.
9. Gordon, D., Martin-Eauclaire, M. F., Cestèle, S., Kopeyan, C., Carlier, E., Khalifa, R. B., Pelhate, M., and Rochat, H. (1996) *J. Biol. Chem. 271*, 8034−8045.
10. Zilberberg, N., Froy, O., Loret, E., Cestèle, S., Arad, D., Gordon, D., and Gurevitz, M. (1997) *J. Biol. Chem. 272*, 14810−14816.
11. Shao, F., Xiong, Y. M., Zhu, R. H., Ling, M. H., Chi, C. W., and Wang, D. C. (1999) *Protein Expression Purif. 17*, 358−365.
12. He, X. L., Li, H. M., Zeng, Z. H., Liu, X. Q., Wang, M., and Wang, D. C. (1999) *J. Mol. Biol. 292*, 125−135.
13. Li, H. M., Wang, D. C., Zeng, Z. H., Jin, L., and Hu, R. Q. (1996) *J. Mol. Biol. 261*, 415−431.
14. Housset, D., Habersetzer-Rochat, C., Astier, J. P., and Fontecilla-Camps, J. C. (1994) *J. Mol. Biol. 238*, 88−103.
15. Xiong, Y. M., Ling, M. H., Wang, D. C., and Chi, C. W. (1997) *Toxicon 35*, 1025−1031.
16. Wu, J. J., He, L. L., Zhou, Z., and Chi, C. W. (2002) *Biochemistry 41*, 2844−2849.
17. Meier, J., and Theakston, R. D. (1986) *Toxicon 24*, 395−401.
18. Kanner, B. J. (1978) *Biochemistry 17*, 1207−1211.
19. Gilles, N., Blanchet, C., Shichor, I., Zaninetti, M., Lotan, I., Bertrand, D., and Gordon, D. (1999) *J. Neurosci. 19*, 8730−8739.
20. Krimm, I., Gilles, N., Sautière, P., Stankiewicz, M., Pelhate, M., Gordon, D., and Lancelin, J. M. (1999) *J. Mol. Biol. 285*, 1749−1763.
21. Gilles, N., Krimm, I., Bouet, F., Froy, D., Gurevitz, M., Lancelin, J. M., and Gordon, D. (2000) *J. Neurochem. 75*, 1735−1745.
22. Cheng, Y., and Prusoff, W. H. (1973) *Biochem. Pharmacol. 22*, 3099−3108.
23. Pelhate, M., and Sattelle, D. B. (1982) *J. Insect Physiol. 28*, 889−903.
24. Hamon, A., Gilles, N., Sautière, P., Martinage, A., Kopeyan, C., Ulens, C., Tytgat, J., Lancelin, J. M., and Gordon, D. (2002) *Eur. J. Biochem. 269*, 3920−3933.
25. Sautière, P., Kopeyan, C., Martinage, A., Drobecq, H., Doljanski, Y., and Gordon, D. (1998) *Toxicon 36*, 1141−1154.
26. Froy, O., Zilberberg, N., Gordon, D., Turkov, M., Gilles, N., Stankiewicz, M., Pelhate, M., Loret, E., Oren, D. A., Shaanan, B., and Gurevitz, M. (1999) *J. Biol. Chem. 274*, 5769−5776.
27. Vargas, O., Martin-Eauclaire, M. F., and Rochat, H. (1987) *Eur. J. Biochem. 162*, 589−599.
28. Cestèle, S., Stankiewicz, M., Mansuelle, P., De Waard, M., Dargent, B., Gilles, N., Pelhate, M., Rochat, H., Martin-Eauclaire, M. F., and Gordon, D. (1999) *Eur. J. Neurosci. 11*, 975−985.
29. Gilles, N., Chen, H., Wilson, H., Le Gall, F., Montoya, G., Heinemann, S. H., and Gordon, D. (2000) *Eur. J. Neurosci. 12*, 2823−2832.
30. He, X. L., Deng, J. P., Wang, M., Zhang, Y., and Wang, D. C. (2000) *Acta Crystallogr. D56*, 25−33.
31. Darbon, H., Jover, E., Couraud, F., and Rochat, H. (1983) *Int. J. Pept. Protein Res. 22*, 179−186.
32. Fontecilla-Camps, J. C., Habersetzer-Rochat, C., and Rochat, H. (1988) *Proc. Natl. Acad. Sci. U.S.A. 85*, 7443−7447.
33. Pintar, A., Possani, L. D., and Delepierre, M. (1999) *J. Mol. Biol. 287*, 359−367.
34. Kharrat, R., Darbon, H., Rochat, H., and Granier, C. (1989) *Eur. J. Biochem. 181*, 381−390.
35. Lecomte, C., Ferrat, G., Fajloun, Z., Van Rietschoten, J., Rochat, H., Martin-Eauclaire, M. F., Darbon, H., and Sabatier, J. M. (1999) *J. Pept. Res. 54*, 369−376.
36. Jover, E., Bablito, J., and Courand, F. (1984) *Biochemistry 23*, 1147−1152.
37. Hansel, A., Lu, S. Q., Leipold, E., and Heinemann, S. E. (2002) *Pfluegers Arch. 443/S02*, P02-2.
38. Tugarinov, V., Kustanovich, I., Zilberberg, N., Gurevitz, M., and Anglister, J. (1997) *Biochemistry 36*, 2414−2424.
39. Catterall, W. A. (1992) *Physiol. Rev. 72*, S15−S48.
40. Gurevitz, M., Gordon, D., Ben-Natan, S., Turkov, M., and Froy O. (2001) *FASEB J. 15*, 1201−1205.
41. Kharrat, R., Darbon, H., Granier, C., and Rochat, H. (1990) *Toxicon 28*, 509−523.
42. Rochat, H., Rochat, C., Sampieri, F., Miranda, F., and Lissitzky, S. (1972) *Eur. J. Biochem. 28*, 381−388.
43. Luo, M. J., Xiong, Y. M., Wang, M., Wang, D. C., and Chi, C. W. (1997) *Toxicon 35*, 723−731.
44. Eitan, M., Fowler, E., Herrmann, R., Duval, A., Pelhate, M., and Zlotkin, E. (1990) *Biochemistry 29*, 5941−5947.
45. Kopeyan, C., Mansuelle, P., Martin-Eauclaire, M. F., Rochat, H., and Miranda, F. (1993) *Nat. Toxins 1*, 308−312.
46. Kopeyan, C., Martinez, G., and Rochat, H. (1978) *FEBS Lett. 89*, 54−58.
47. Kraulis, P. J. (1991) *J. Appl. Crystallogr. 24*, 946−950.
48. Merrit, E. A., and Bacon, D. J. (1997) *Methods Enzymol. 277*, 505−524.

BI0270438